Myosin V Plays an Essential Role in the Thyroid Hormone-dependent Endocytosis of Type II Iodothyronine 5′-Deiodinase*

Stanley J. Stachelek‡, Tim F. Kowalik§, Alan P. Farwell‡, and Jack L. Leonard‡¶

From the ‡Department of Cellular and Molecular Physiology and the §Department of Molecular Genetics and Microbiology, University of Massachusetts Medical School, Worcester, Massachusetts 01655

In astrocytes, thyroxine modulates type II iodothyronine 5′-deiodinase levels by initiating the binding of the endosomes containing the enzyme to microfilaments, followed by actin-based endocytosis. Myosin V is a molecular motor thought to participate in vesicle trafficking in the brain. In this report, we developed an *in vitro* actin-binding assay to characterize the thyroid hormone-dependent binding of endocytotic vesicles to microfilaments. Thyroxine and reverse triiodothyronine (EC_{50} levels ~1 nM) were >100-fold more potent than 3,5,3′-triiodothyronine in initiating vesicle binding to actin fibers *in vitro*. Thyroxine-dependent vesicle binding was calcium-, magnesium-, and ATP-dependent, suggesting the participation of one or more myosin motors, presumably myosin V. Addition of the myosin V globular tail, lacking the actin-binding head, specifically blocked thyroid hormone-dependent vesicle binding, and direct binding of the myosin V tail to enzyme-containing endosomes was thyroxine-dependent. Progressive NH_2-terminal deletion of the myosin V tail and domain-specific antibody inhibition studies revealed that the thyroxine-dependent vesicle-tethering domain was localized to the last 21 amino acids of the COOH terminus. These data show that myosin V is responsible for thyroid hormone-dependent binding of primary endosomes to the microfilaments and suggest that this motor mediates the actin-based endocytosis of the type II iodothyronine deiodinase.

Type II iodothyronine deiodinase (D2)[1] is a membrane-bound enzyme that catalyzes the generation of T_3 from T_4, and is the major source of T_3 in brain, pituitary, and brown adipose tissue (1, 2). In the brain, D2 levels are dynamically regulated by thyroid hormone (3–6). The thyroid hormone-dependent regulation of D2 observed *in vivo* is mimicked in cAMP-stimulated astrocytes in culture (4). In the absence of thyroid hormone, D2 levels are elevated, enzyme turnover is slow, and the microfilaments are disrupted (4, 7). Addition of T_4 or rT_3, but not the transcriptionally active T_3, causes the rapid restoration of the microfilaments and activates actin-based endocytosis of D2-containing vesicles, leading to a rapid fall in D2 levels in the cell activity (5, 8, 9). Importantly, repolymerization of the microfilaments in the absence of thyroid hormone does not alter D2 turnover or activate the actin-based endocytosis of D2-containing vesicles (5, 8, 9), suggesting that thyroid hormone independently regulates actin-based endocytosis. Inhibitor studies showed that disruption of the actin cytoskeleton by dihydrocytochalasin or depletion of cellular ATP stores block the T_4-induced loss of D2 (4, 5) indicating that intact microfilaments and an energy source are required for the dynamic regulation of the turnover of this membrane-bound enzyme.

One of the first steps in the T_4-dependent regulation of astrocyte D2 activity is the hormone-induced binding of D2-containing vesicles to filamentous actin (F-actin). This is rapidly followed by the translocation of the actin-bound vesicle to the perinuclear space (5, 10). Myosin motor proteins mediate the translocation of vesicle on actin fibers. Myosins comprise a superfamily of actin-binding, Mg^{2+}-ATPase, motor proteins (11), and unconventional myosins are found in virtually all cell types, where they participate in cell contraction, cell motility, and vesicle trafficking (12). Four unconventional myosin family members (I, V, VI, and VII) have been reported to participate in membrane trafficking (12, 13). Myosin V is the most abundant of this subset in brain, where it is found to be associated with vesicles in nerve terminals (13, 14). Myosin V forms calcium-dependent complexes with the synaptic vesicle proteins, synaptobrevin and synaptophysin (14). Although this motor protein does not appear to associate with the mature synaptic vesicle, ultrastructure analysis showed that larger-sized, SV2-positive vesicles in the synapse were decorated with myosin V (15), suggesting that myosin V is bound to endosomes and/or to recycling synaptic vesicles (16).

In this study, we examined the participation of myosin V in the thyroid hormone-dependent binding of D2-containing vesicles to the actin cytoskeleton. Using both the native, affinity-radiolabeled D2, and exogenous expression of a GFP-tagged D2 fusion protein, we show that an actin-bound protein with calcium-dependent ATPase activity tethers the D2-containing endosome to F-actin. Deletion analysis and antibody inhibition studies showed that the COOH-terminal 21 amino acids anchored the D2 vesicle to the myosin motor in a hormone-dependent manner. These data suggest that the processive myosin V motor participates in the T_4-dependent actin-based endocytosis of D2.

¶ To whom correspondence should be addressed: Dept. of Cellular and Molecular Physiology, University of Massachusetts Medical School, 55 Lake Ave. North, Worcester, MA 01655. Tel.: 508-856-6687; Fax: 508-856-4572; E-mail: jack.leonard@umassmed.edu.

[1] The abbreviations used are: D2, type II iodothyronine deiodinase; p29, 29-kDa substrate binding subunit of D2; BrAc[^{125}I]T_4, *N*-bromoacetyl-L-[^{125}I]thyroxine; T_4, thyroxine; T_3, 3′,3,5-triiodothyronine; rT_3, 3′,5′,3-triiodothyronine; KLH, keyhole limpet hemacyanin; GFP, green fluorescence protein; PAGE, polyacrylamide gel electrophoresis; HRP, horseradish peroxidase; SV2, synaptic vesicle protein 2; TEMED, *N,N,N′,N′*-tetramethylethylenediamine; bp, base pair(s); DMEM, Dulbecco's modified Eagle's medium.

EXPERIMENTAL PROCEDURES

Materials— T$_4$, Triton X-100, ATP, Bt$_2$cAMP, hydrocortisone, colchicine, bovine serum albumin, and rabbit anti-actin IgG were obtained from Sigma (St. Louis, MO). DMEM, antibiotics, Hanks' solution, and trypsin were purchased from Life Technologies, Inc. (Gaithersburg, MD). Acrylamide was purchased from National Diagnostics (Atlanta, GA). TEMED and ammonium persulfate were purchased from Bio-Rad (Richmond, CA). Hybond ECL nitrocellulose was obtained from Amersham Pharmacia Biotech (Arlington Heights, IL); horseradish peroxidase (HRP)-conjugated goat, anti-rabbit IgG was obtained from Promega (Madison, WI); rabbit anti-GFP IgG was from CLONTECH (Palo Alto, CA). The Lumiglo chemiluminescent detection system was obtained from Kirkegaard and Perry (Gaithersburg, MD). BrAc[^{125}I]T$_4$ was synthesized as described previously (17). The TNT-coupled transcription-translation kit was purchased from Promega (Madison, WI). Restriction endonucleases and DNA-modifying enzymes were purchased from New England BioLabs (Beverly, MA).

Culture Conditions—Astrocytes were prepared from 1-day-old neonatal rats as described previously (18) and grown in growth medium composed of DMEM supplemented with 10% supplemented bovine calf serum, 50 units/ml penicillin, and 90 units/ml streptomycin. Cells were grown to confluence in 75-cm^2 culture flasks in a humidified atmosphere of 5% CO$_2$ and 95% air at 37 °C and used at passages 1–3.

Actin Binding Assay—Cell lysates with intact microfilaments (F-lysate) were prepared from thyroid hormone-deficient astrocytes treated for 24 h with 10 μM retinoic acid in serum free media as detailed previously (10). Cell lysates with BrAc[^{125}I]T$_4$-labeled p29 vesicles (V-lysate) were prepared from cAMP-stimulated astrocytes in serum free media that were labeled with 2 nM BrAc[^{125}I]T$_4$ as described previously (5). Microtubules were depolymerized in all cells using 10 μM colchicine for 30 min before cell isolation. Cells were then scraped from the flask, collected by centrifugation (500 × g for 5 min), washed with phosphate-buffered saline (pH 7.4), and the cell pellets were lysed by two freeze-thaw cycles (5, 8). Lysates could be stored at −70 °C for up to 4 weeks without loss of hormone-dependent actin binding. F- and V-lysates (100 μg of cell protein each) were combined on ice, 10 nM T$_4$, 10 nM rT$_3$, or 10 nM T$_3$ were added, and the mixtures were incubated for 20 min at 37 °C. Mixtures were then chilled on ice for 2 min, Triton X-100 (0.5% v/v, final concentration) was added, and the soluble (Triton supernatant) and particulate (Triton pellet) fractions were separated by centrifugation at 4 °C for 65,000 × g·min. The distribution of ^{125}I-labeled p29 between the Triton supernatant and Triton pellet was determined by SDS-PAGE analysis.

Antibody Preparation—Synthetic peptides corresponding to the last 22 amino acids COOH-terminal to myosin V (NH$_2$-YSLALETIQIPASL-GLGFIARV-COOH) were synthesized by the Peptide Synthesis Core at the University of Massachusetts Medical School. An NH$_2$-terminal tyrosine was added to facilitate diaminobenzidine coupling to KLH and for radioiodination. The peptide-KLH conjugate (750 μg of KLH conjugate/500 μl) was mixed with an equal volume of complete Freund's adjuvant and injected intradermally at 20 sites on the back of 2.2-kg female New Zealand white rabbits. Antibodies were also raised against an internal myosin V domain corresponding to the last IQ domain and the coiled-coil region (residues 892 to 1040, myosin V^{mid}). Polymerase chain reaction amplified myosin V cDNA was prepared using site-specific, 20-mer oligonucleotides and the ~800-bp fragment was cloned into the *Eco*RV site of the pThioHis B prokaryotic expression vector (Invitrogen, San Diego, CA). The fusion protein was synthesized in isopropyl-1-thio-β-D-galactopyranoside-induced *Escherichia coli*. The myosin V^{mid} fusion protein was purified on Ni-Sepharose from cell lysates according to the manufacturer's instructions. Approximately 75 μg of myosin V^{mid} was diluted 50:50 with complete Freund's adjuvant used to immunize rabbits as described above.

The specificity of the two rabbit anti-myosin V antisera was documented by immunoblot analysis. Brain homogenates were prepared from normal, heterozygous (myosin V$^{+/-}$) and myosin V-deficient, homozygous *dilute* mouse (myosin V$^{-/-}$). Both antibodies recognized a 190-kDa protein in the brain homogenates containing myosin V (heterozygotes) but showed no immunoreactive band in the homogenates of *dilute* mouse brain that lacks myosin V (Fig. 1).

Immunoblotting—Total cell protein was measured by the Bradford dye binding assay (Sigma), and 20–50 μg of cellular protein was reduced, denatured, and separated by SDS-PAGE according to the method of Laemmli (19). Resolved proteins were transferred to Hybond membranes by electrotransfer using a semidry transfer apparatus (200 mA for 1 h). The membrane was blocked in Tris-buffered saline (pH 7.5) containing 0.1% Tween 20 (v/v) and 5% powdered milk (w/w). Immuno-
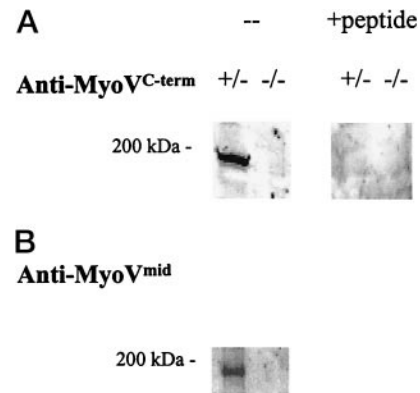
FIG. 1. **Characterization of rabbit polyclonal antibodies raised against myosin V.** 50-μg aliquots of myosin V enriched vesicle protein prepared from cerebella of normal (±) or *dilute lethal* (−/−) mice were separated on a 5% SDS-PAGE gel and transferred to Hybond. Blots were probed with antibodies specific for the COOH terminus (*A*) or the coiled-coil (*B*) region of myosin V ± 10 μg/ml blocking peptide, as indicated. Immune complexes were detected by chemiluminescence as described under "Experimental Procedures."

blots were then probed with primary antibodies (1:500 for anti-myosin V antisera; 2 μg/ml for anti-GFP IgG) for 16 h at 4 °C. After washing, immune complexes were detected with HRP-conjugated, goat, anti-rabbit IgG (1:2000 final dilution), and the specific complexes were visualized by chemiluminescence and Kodak X-Omat AR5 radiographic film.

Construction of Replication-deficient, Myosin V Viral Vectors—The 3280-bp fragment containing the coding sequence of the globular myosin V tail cDNA (myosin V^{tail}) was excised from clone D64 (a gift from Dr. Nancy Jenkins, National Cancer Institute, Frederick, MD) with *Ssp*I and *Eco*47III and ligated into the *Eco*RV site of the AdpREC shuttle vector. The shuttle construct was linearized with *Eco*RI and cotransfected with *Xba-Cla*I linearized Ad5-βgal into HEK 293 cells using Lipofect AMINE according to the manufacturer's instructions. Replication-deficient Ad5-myoV-containing virus particles were purified from the HEK-293 cell lysates by cesium chloride gradient centrifugation. Expression of myosin V from Ad5-myoV-infected cells was confirmed by Western blot analysis. The Ad5-p29^{GFP} virus particles were generated as detailed previously (20).

Immunocytochemistry—Astrocytes were seeded onto poly-d-lysine (10 μg/ml)-coated coverslips and grown for 24–48 h in growth medium. Medium was changed to serum-free DMEM ± 10 nM T$_4$ and treated with 1 mM Bt$_2$cAMP, 10 μM all-*trans*-retinoic acid, and 100 nM hydrocortisone for 16 h. Microtubules were depolymerized with 10 μM colchicine for 30 min before fixation. Cells were fixed with 4% paraformaldehyde and permeabilized with 0.1% Triton X-100. Cells were then incubated with anti-myosin V antisera (COOH terminus, 1:500), and immune complexes were visualized using a Texas Red-conjugated, anti-rabbit IgG. Images were collected by digital imaging microscopy in the Biomedical Imaging Facility at the University of Massachusetts Medical School. 20–50 random fields were examined per treatment group.

Statistics—All experiments were done a minimum of three times, and, where appropriate, statistical analysis was performed using Student's *t* test.

RESULTS

Myosin V Is Present in Astrocytes in Culture—Myosin V comprises ~0.3% of total protein in brain. To determine the myosin V content in cultured astrocytes, we examined untreated and T$_4$-treated cells for the presence and distribution of myosin V using Western blot analysis and immunocytochemistry. As shown in Fig. 2*A*, >90% of the 190-kDa, immunoreactive myosin V was found in the Triton-insoluble pellets prepared from retinoid-treated astrocytes in the absence or presence of T$_4$. Preincubation of the anti-myosin V antibody with excess blocking peptide (10 μg/ml) eliminated the 190-kDa immunoreactive band (see Fig. 1), indicating that the myosin V present in astrocytes is predominantly associated with the F-actin cytoskeleton. Also shown in Fig. 2*A* is the distribution of immunoreactive actin between the Triton supernatant and
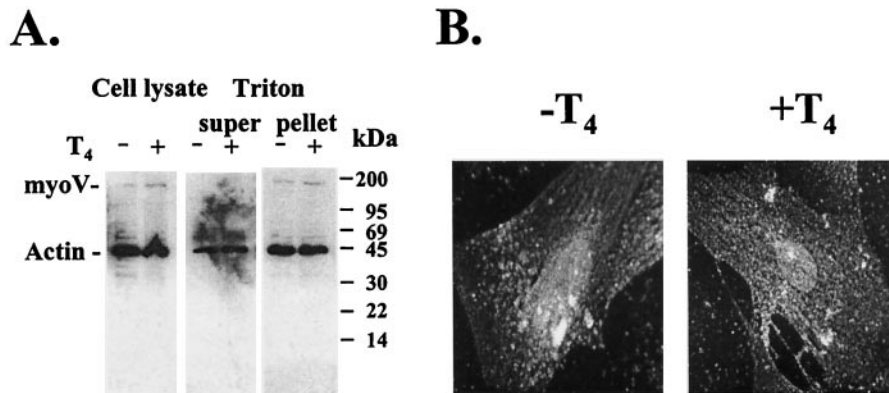
FIG. 2. **Characterization of distribution of actin and myosin V in Triton soluble and insoluble fractions from cultured astrocytes.** *A*, immunoblot. Cultured astrocytes were treated overnight with 10 μM retinoic acid $\pm$ 10 nM T_4. Cells were collected, and Triton X-100 supernatants and pellets were prepared as described under "Experimental Procedures." Equivalent volumes of resuspended Triton pellet, Triton supernatant, and whole cell lysate were separated on 5–20% linear gradient SDS-PAGE gels and transferred to nitrocellulose. Immunoblot analysis for both myosin V and actin was done simultaneously, using rabbit, anti-myosin V antisera (1:500 final dilution) and rabbit, affinity purified anti-actin IgG (8 μg/ml). After washing, immune complexes were visualized using HRP-conjugated goat, anti-rabbit IgG (1:2000 final dilution) as described under "Experimental Procedures." *B*, photomicrographs of the distribution of myosin V in retinoid-treated astrocytes grown in the absence and presence of 10 nM T_4. Cell treatments and immunohistochemistry were done as described under "Experimental Procedures."

Triton pellet from retinoid-treated astrocytes that were grown in the absence and presence of T_4. No differences in total actin content were observed, and >90% of the immunoreactive actin was found in the Triton-insoluble pellet in both thyroid hormone-deficient and T_4-treated cells as determined by densitometry (data not shown). In control experiments, no specific immune complexes were observed in the 200-kDa range of immunoblots of astrocyte cell lysate, indicating that the anti-actin IgG did not cross-react with myosin V (data not shown). These data illustrate that, as reported previously (10), the retinoid-treated, thyroid hormone-deficient astrocyte contained a fully polymerized actin cytoskeleton and indicate that myosin V is constitutively bound to F-actin. Fig. 2*B* shows representative photomicrographs of the cellular distribution of immunoreactive myosin V in retinoid-treated astrocytes treated in the absence and presence of 10 nM T_4. Specific immunoreactive myosin V was found distributed throughout the cell in linear arrays and punctate clusters both in the absence and in the presence of T_4. These data show that astrocytes express abundant myosin V and that thyroid hormone does not affect the distribution of myosin V in the cell.

In Vitro Actin Binding Assay: Hormone-dependent Binding of p29 Vesicles to F-actin—T_4 specifically promotes the rapid redistribution of affinity-labeled p29 between the Triton-soluble and Triton-insoluble fractions in living cells (10). We exploited this to develop an *in vitro* binding assay to identify the components that mediate the hormone-dependent binding of the p29-containing vesicles to F-actin. Two different pools of astrocytes were prepared: one, the F-lysate, provided fully polymerized F-actin with its associated myosin V and was prepared by treating thyroid hormone-deficient astrocytes with 10 μM retinoic acid as described previously (10). The other, V-lysate, provided the affinity-labeled p29 vesicles in thyroid hormone-deficient astrocytes (5). Fig. 3 shows a representative fluorograph of the effects of thyroid hormone on the distribution of affinity-labeled p29 vesicles in our *in vitro* actin-binding assay. As expected, comparable levels of affinity-labeled p29 were present in the lysate mixtures, as judged by the intensity of the lower band of the doublet of radiolabeled proteins at a region of ~30 kDa (21). In the absence of hormone, >90% of the affinity-labeled p29 was found in the Triton supernatant. Addition of 10 nM T_3 to the mixed cell lysates had no effect on the distribution of affinity-labeled p29, because >90% of the affinity-labeled p29 remained in the Triton-soluble fraction. In contrast, addition of 10 nM T_4 to the mixed cell lysates resulted in the binding
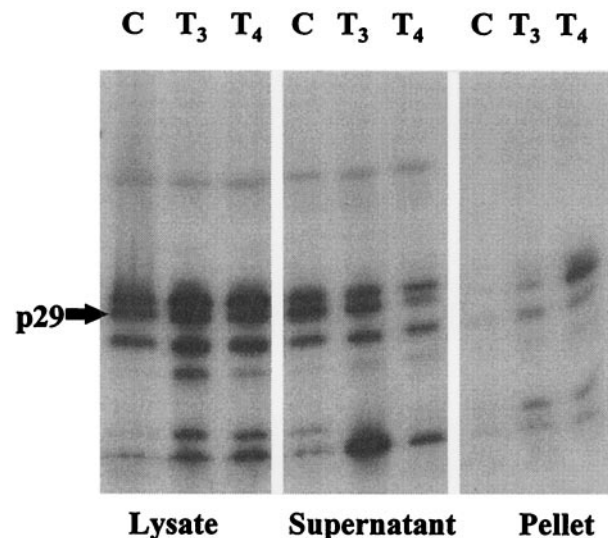
FIG. 3. **Thyroid hormone-dependent attachment of the BrAc[^{125}I]T_4-labeled p29 vesicles to F-actin *in vitro*.** V- and F-lysates were prepared as described under "Experimental Procedures." Mixtures were treated with no hormone, 10 nM T_3, or 10 nM T_4 for 20 min, and the Triton-soluble and -insoluble F-actin cytoskeleton was separated by centrifugation. Proteins were resolved by SDS-PAGE, and the distribution of radiolabeled proteins was determined by fluorography

of >70% of the affinity-labeled p29 to the Triton-insoluble, F-actin fraction. These data show that the T_4-dependent binding of the p29 vesicle to the actin cytoskeleton in a broken cell preparation mimics that observed in the living astrocyte (5).

The Binding of p29 to the Actin Cytoskeleton Is Calcium-, Magnesium-, and ATP-dependent—Although the *in vitro* actin binding assay showed that T_4 can initiate the binding of p29 endosomes to F-actin, whether this is a direct interaction between the vesicle and F-actin or is mediated by other actin-bound proteins, such as myosin V, remains to be established. A characteristic of myosin V is the ability to release the motor from F-actin by activating the Ca^{2+}-dependent Mg-ATPase found in the actin binding head of myosin V (14, 22). We next examined whether activating the Ca^{2+}-dependent Mg-ATPase would release p29 vesicles bound to F-actin. Equal volumes of F-lysate and V-lysate were mixed, and p29 vesicle:F-actin binding was initiated by adding 10 nM T_4 for 20 min. The reconstituted lysates were then treated with 0.1 mM Ca^{2+}, 1 mM Mg^{2+},
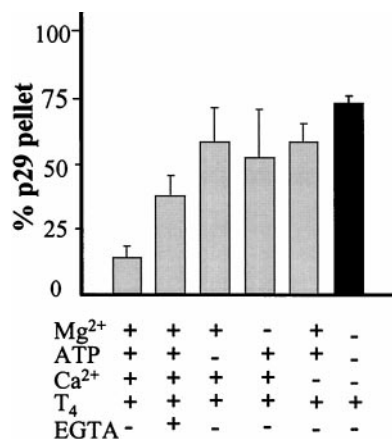
FIG. 4. **Calcium, ATP-dependent interactions between the p29 subunit of D2 and the F-actin cytoskeleton.** Confluent monolayers of astrocytes were grown in serum-free media for 16 h. D2 activity was induced with Bt$_2$cAMP and hydrocortisone, and the p29 vesicle was affinity radiolabeled with BrAc[^{125}I]T$_4$. Cell lysates containing ~50,000 cpm of BrAc[^{125}I]T$_4$-labeled p29 were pretreated with 10 nM T$_4$ for 20 min at 37 °C, followed by an additional 20 min with 0.1 mM Ca^{2+}, 1 mM Mg^{2+}, 0.1 mM ATP, or 5 mM EGTA as indicated. Triton-insoluble (F-actin bound) pellets were prepared as described under "Experimental Procedures." Proteins were separated on 12.5% SDS-PAGE gels, and the p29 content was determined by phosphorimaging using a Molecular Dynamics PhosphorImager.

0.1 mM ATP, and/or 5 mM EGTA as indicated and incubated for an additional 30 min at 37 °C. Triton-insoluble pellets were separated from the Triton-soluble fraction, and the distribution of p29 was determined.

As shown in Fig. 4, ~80% of the total p29 vesicles added were bound to F-actin at the start of the experiment. Activation of Ca^{2+}-dependent Mg-ATPase(s) by the addition of divalent ions (Ca^{2+} and Mg^2) and ATP resulted in the release of ~70% of the p29 vesicles from F-actin without altering the F-actin content in the Triton pellet. The calcium chelator, EGTA, blocked >50% of release of p29 from F-actin. Similarly, removing the substrate, ATP, or either divalent ion completely blocked the release of p29 vesicles from F-actin. These data suggest that myosin motor protein(s), presumably myosin V, participate in the binding of the p29 vesicle to F-actin.

Characterization of the Interaction(s) between the Myosin V Tail and p29 Vesicles—Although the actin binding region of myosin V is located at the NH$_2$ terminus of the protein, the vesicle binding region of myosin V appears to be located in the unique ~80-kDa globular tail (14). In the next series of studies, we generated truncation mutants of myosin V that lack the actin-binding head and examined the ability of these myosin V tail mutants to compete with the native, F-actin-bound myosin V for the p29 vesicles. Initial studies used the entire COOH terminus of myosin V synthesized *in vitro* from a 4.2-kb fragment (nucleotide 2911–7087) of the myosin V cDNA (Δ myosin V^{tail}) using the coupled transcription and translation system (TNT, Promega). Cell-free synthesis of the appropriate myosin V mutant was confirmed by immunoblot, and an 88-kDa band was detected using anti-myosin V antibodies directed against the COOH-terminal 21 amino acids (Fig. 5, *inset*). Increasing volumes (5 or 10 μl) of Δ myosin V^{tail} or a comparable volume of control reticulocyte lysate were added to the *in vitro* actin binding assay and preincubated for 20 min at 37 °C. Actin binding of the p29 vesicles was then initiated by 10 nM T$_4$. As illustrated in Fig. 5, addition of 5 μl of Δ myosin V^{tail} blocked ~50% of the T$_4$-dependent binding of p29 vesicles to F-actin, whereas 10 μl of Δ myosin V^{tail} blocked >95% of the p29 binding. In control actin binding assays, addition of up to 10 μl of the reticulocyte lysate failed to affect the T$_4$-dependent p29
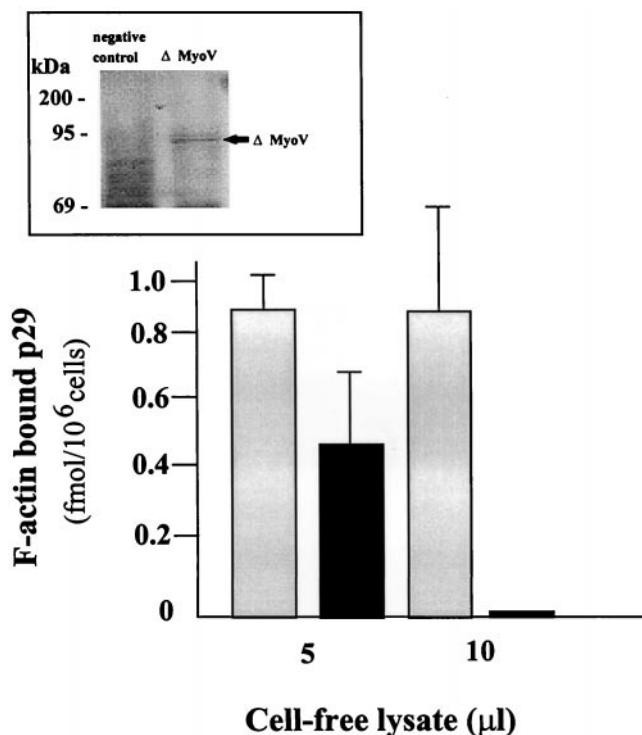
FIG. 5. **Effects of truncated myosin V on the binding of p29 vesicles to F-actin.** The ~88-kDa COOH terminus of myosin V was synthesized *in vitro* from a 4.2-kb fragment (nucleotide 2911–7087) of the myosin V cDNA using the TNT-coupled transcription and translation system. Correct synthesis was confirmed by immunoblot using an anti-myosin V IgG raised to the coiled-coil region of myosin V (*inset*). Increasing volumes (5 or 10 μl) of cell-free-translated myosin V tail (*solid*) or control reticulocyte lysate (*gray*) was added to the actin binding reconstitution assay. Actin binding of the p29 vesicle was initiated by the addition of 10 nM T$_4$. F-actin bound p29 was determined as described under "Experimental Procedures." Data are reported as means of triplicate determinations.

vesicle binding to F-actin. These data indicate that the tail region of myosin V competes with the wild type motor and blocks the T$_4$-dependent binding of p29 vesicles to F-actin.

Based on the dominant negative effect of the Δ myosin V tail on p29 vesicle binding *in vitro*, we created a series of deletion mutations to define the specific region(s) of myosin V tail that interact with the p29 vesicle. To simplify the analysis of the competition of the myosin V deletion mutations on T$_4$-dependent binding of p29 vesicles to F-actin, we modified the *in vitro* assay by replacing the affinity-labeled p29 with a GFP-tagged p29 fusion protein (p29^{GFP}) (5, 8). This allowed direct evaluation of the binding of fluorescent vesicles to F-actin without affinity labeling of the p29 or SDS-PAGE analysis. Exogenous p29^{GFP} was introduced into the astrocytes used to prepare the V-lysate by infection with replication-deficient Ad5-p29^{GFP} virus particles. 48 hours after infection, >99% of the infected astrocytes expressed the p29^{GFP}. Cells expressing the p29^{GFP} were then used to prepare the V-lysate as described under "Experimental Procedures". Equal volumes of F-lysate and V-lysate containing p29^{GFP}-labeled vesicles were incubated with increasing concentrations of T$_4$, rT$_3$, or T$_3$ (0–100 nM) for 20 min at 37 °C, and the quantity of p29^{GFP} in the Triton pellets was determined by fluorometry. Fig. 6 shows representative dose-response curves for thyroid hormone-dependent p29^{GFP} vesicle binding to F-actin. As expected, both T$_4$ and rT$_3$ initiated increases in the quantity of p29^{GFP} bound to the F-actin with EC$_{50}$ values of ~1 nM, in close agreement to those reported previously (10). T$_3$ had little, if any, effect on p29^{GFP} vesicle binding to F-actin, except for a modest 10–20% effect observed
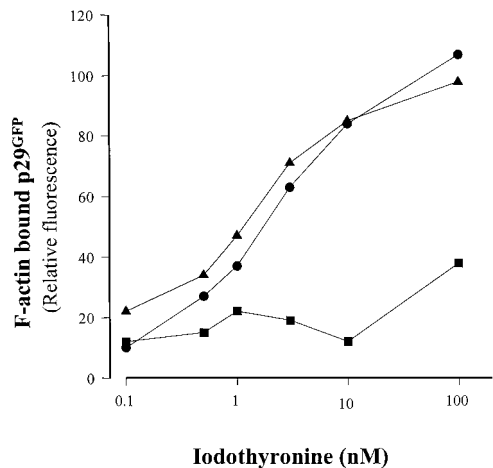
FIG. 6. Hormone-dependent association between p29^GFP-containing vesicles and F-actin. Astrocytes expressing p29^GFP were grown in serum-free media and treated for 16 h with 1 mM Bt₂cAMP and 100 nM hydrocortisone. A separate pool of astrocytes was treated in serum-free media supplemented with 10 μM retinoic acid. Cells were collected by scraping and lysed by two freeze-thaw cycles. 100-μg aliquots of p29^GFP V-lysate and F-lysate were incubated, in triplicate, for 20 min with increasing concentrations of (●) T₄, (■) T₃, or (▲) rT₃. Triton-soluble (vesicle) and -insoluble (F-actin) fractions were separated by centrifugation. Triton pellets were resuspended in 300 μl of PBS, and fluorescence at 510 nm (excitation 488 nm) was determined. Relative fluorescence is reported as arbitrary units, and the data are expressed as means of closely agreeing (±10) triplicates.
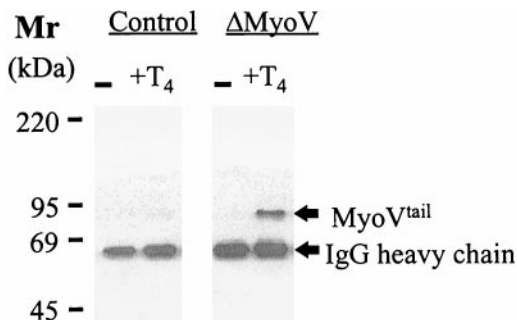
FIG. 7. T₄-dependent binding of the COOH terminus of myosin V to p29 vesicles. Astrocytes constitutively expressing p29^GFP were infected with Ad5-ΔMyoV^tail (multiplicity of infection, 10:1) 48 h before the start of the experiment. Growth medium was replaced with T₄-free, defined medium, and the cells were treated with 1 mM Bt₂cAMP and 100 nM hydrocortisone for 16 h. Control (no ΔMyoV^tail) and ΔMyoV^tail-expressing cells were then treated with 10 nM T₄ for 20 min; the cells were harvested by scraping and collected by centrifugation. Cells were resuspended in lysis buffer containing 0.1% Triton (v/v), and clarified extracts were prepared by centrifugation. 100 μl of clarified extract was then incubated for 90 min ± 2 μg/ml anti-GFP IgG, and 10 μl of Protein A-Immunobeads. The Immunobeads were collected and washed, and the bound proteins were eluted with 2× Laemmli sample buffer. Eluted proteins were separated on 10% SDS-PAGE gels and transferred to Hybond ECL. Immunoreactive myosin V polypeptides were identified by anti-myosin V IgG (1:500) directed against the COOH terminus of rat myosin V, as described under "Experimental Procedures." Note the large residual band of IgG heavy chain recognized by the secondary antibody.

at 100 nM T₃, the highest concentration of hormone used.

To determine if the Δ myosin V tail was directly bound to the p29 vesicle, we introduced a Δ myosin V^tail into p29^GFP-expressing astrocytes by infection with Ad5-ΔmyoV^tail virus particles and examined the effects of T₄ on the binding of the myosin V^tail to immunopurified p29^GFP vesicles. Cells were treated with or without 10 nM T₄ for 20 min, and the cell was lysed with 0.1% Triton. Vesicles containing the p29^GFP in the clarified extract were immunoprecipitated by anti-GFP IgG (2
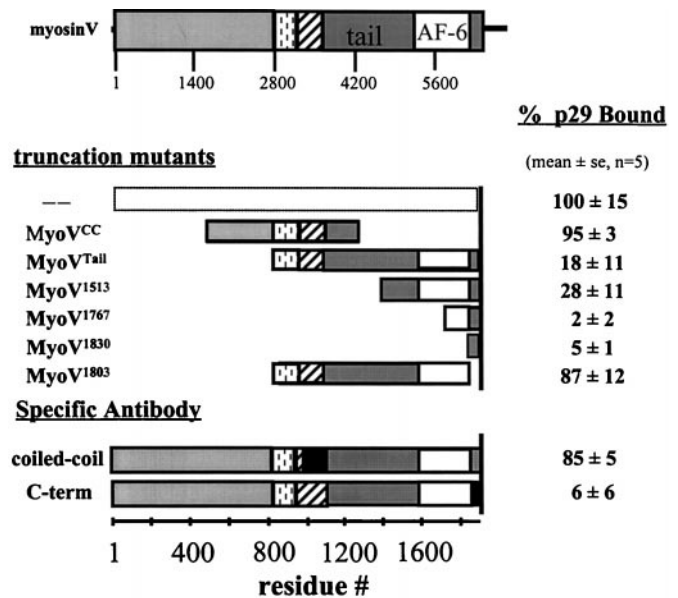
FIG. 8. Characterization of myosin V deletion mutants on the attachment of p29^GFP to F-actin. Astrocytes expressing p29^GFP were grown in serum-free media and treated for 16 h with 1 mM Bt₂cAMP and 100 nM hydrocortisone. p29^GFP V-lysate and F-lysate were prepared as described under "Experimental Procedures." 100-μg aliquots of p29^GFP V-lysate and F-lysate were preincubated, in triplicate, for 20 min at 37 °C ±10 μl of individual myosin V deletion mutant, followed by an additional 20 min with 10 nM T₄. Triton-soluble (vesicle) and -insoluble (F-actin) fractions were separated by centrifugation. F-actin-bound p29^GFP vesicles were measured as described in the legend to Fig. 7. Data are expressed as the percentage of the maximal Triton-insoluble fluorescence observed in the absence of myosin V mutants and reported as means ± SE of three separate experiments. ▦, actin binding head; ▨, neck; ▧, coiled-coil; ▤, tail; ■, epitope.

μg/ml), and those in the immunoprecipitated vesicles were resolved by SDS-PAGE. Shown in Fig. 7 is a representative immunoblot of Δ myosin V^tail associated with affinity-purified vesicles from control p29^GFP cells and from p29^GFP cells expressing the Δ myosin V^tail. In control cells, no myosin V immunoreactive protein(s) was detected in the purified vesicle pool, because the native, F-actin bound myosin V was removed during clarification. In contrast, the Δ myosin V^tail showed a T₄-dependent association with the p29^GFP vesicle, as judged by the co-purification of this 88-kDa immunoreactive band. These data show that the direct interaction between the p29 vesicle and myosin V is T₄-dependent.

In Vitro Analysis of the Effects of Myosin V Truncation Mutants on T₄-dependent p29 Binding to F-actin—Fig. 8 shows a schematic diagram of the myosin V^tail deletion mutations studied. All deletion mutants were synthesized by cell-free translation, and the synthesis of the correct myosin V polypeptide was confirmed by Western blot analysis (data not shown). The quantity of each mutant protein synthesized was determined by [³⁵S]met incorporation and ranged from 400 to 1000 ng/reaction (data not shown). Individual Δ myosin V mutant proteins (~2–3 pmol of polypeptide/50 μl of mixture) were added to the actin-binding assay and preincubated for 20 min at 37 °C. T₄ (10 nM) was added, the mixtures were incubated for an additional 20 min, and the F-actin-bound, fluorescent p29^GFP vesicles were then isolated in the Triton-insoluble pellet.

Data reported in Fig. 8 are expressed as the percentage of the maximum, T₄-dependent p29 vesicle binding observed in the absence of added competitors. Addition of the Δ myosin V^mid protein, corresponding to amino acids 504–1307, did not compete with native myosin V for the T₄-dependent binding of p29 vesicles to F-actin (*p* = NS). As observed above (see Fig. 5), addition of the entire myosin V^tail (residues 953–1852) de-

creased p29 binding to F-actin by >80% ($p < 0.01$). Addition of progressively shorter myosin V^{tail} deletion mutants: Δ myosin^{1513} (residues 1513–1852), Δ myosin^{1767} (residues 1767–1852), and Δ myosin^{1830} (residues 1830–1852) all competed with native myosin V and significantly decreased T_4-dependent p29 binding from 75% to 98% ($p < 0.01$). However, the Δ myosin V tail lacking only the last 44 residues (residues 953–1803) did not compete with native myosin V for T_4-dependent p29 vesicle binding. These data indicate that the T_4-dependent, vesicle-binding region of myosin V is located within the last 21 amino acids at the COOH terminus of the motor protein.

Antibodies Directed Against the C Terminus of Myosin V Block the T_4-dependent Binding of p29 Vesicles to F-actin— Antibody inhibition studies were done to confirm the location of the vesicle-tethering region of myosin V. Two antibodies were used; one raised against the coiled-coil domain (residues 892–1040), and one directed against the COOH-terminal 21 amino acids (residues 1831–1852). The data summarized in Fig. 8 indicate that antibodies that are directed against the extreme COOH terminus of myosin V completely block the T_4-dependent binding of p29 vesicles to F-actin, whereas antibodies that are directed against the coiled-coil domain failed to alter p29 vesicle binding to F-actin. Control rabbit immunoglobulins had no effect of the T_4-dependent binding of p29 vesicles to myosin V (data not shown). These data confirm the assignment of the vesicle-tethering domain to the COOH terminus of myosin V.

Finally, we examined the possibility of a direct interaction between myosin V and T_4. 2–3 pmol of cell-free-translated Δ myosin V^{tail} was incubated with 0.2 nM ^{125}I-labeled 3'- or 5'-T_4 (50,000 cpm) in the absence or presence of 10 μM T_4 for 90 min at room temperature. No significant binding of T_4 to myosin V was observed under these conditions, indicating that myosin V is not a T_4 binding protein.

DISCUSSION

In this study we show that a vesicle-tethering domain located at the COOH terminus of the unconventional myosin motor protein, myosin V, mediates the thyroid hormone-dependent attachment of endosomes to F-actin. The participation of myosin V in vesicle trafficking is well known (12, 14, 23). This motor protein has been shown to move vesicles along actin fibers *in vitro* (15, 24), and loss of myosin V in yeast and in mice leads to profound defects in cell migration, vesicle trafficking, and oriented organelle transport (25–27). In mice, *dilute* mutants show a lightened coat color and severe neurological defects that result in large part from aberrant vesicle transport and impaired cell migration, even though the actin cytoskeleton is unaffected (28, 29). In yeast, mutants of Myo2p, a class V myosin motor, show impaired vacuole transport and loss of polarized movement of membrane-limited organelles (27). The ability of myosin V to dock with intracellular vesicles and tether these organelles to actin filaments is central to the function of this motor protein (30, 31) and also to the ability of myosin V to participate in the thyroid hormone-dependent endocytosis of D2 in brain.

Using a straightforward *in vitro* actin-binding assay, we showed that the binding of D2-containing endocytotic vesicles to F-actin was regulated by thyroid hormone. *In situ*, both T_4 and rT_3, two transcriptionally inert thyroid hormones, initiate the actin-based endocytosis of the membrane-bound, short-lived, enzyme D2 (4, 5), mimicking events observed in brain *in vivo* (6). *In vitro*, the binding of D2 vesicles to F-actin showed the same iodothyronine specificity found in cAMP-stimulated astrocytes *in situ* (10) and in the brain *in vivo* (6). In cAMP-stimulated astrocytes, myosin V is tightly bound to the microfilaments, and activation of Ca^{2+}-dependent MgATPase(s), presumably the catalytic activity associated with the actin-

binding head of the endogenous myosin V, released the D2-containing vesicles from F-actin. These findings are similar to those of others (14, 22) who found that addition of Ca^{2+}, Mg^{2+}, and ATP optimized the release of vesicles tethered to F-actin by myosin V, presumably by activating the ATPase. In contrast to the observations made with native, full-length myosin V, the Ca^{2+}-dependent MgATPase activity, associated with myosin V fragments lacking the neck and tail domains but retaining the actin binding head, is blocked by calcium and shows a different affinity for F-actin (32). Presumably, the loss of light chains and/or other accessory proteins accounts for the differences in the effects of Ca^{2+} on the interactions between the myosin V head and F-actin. Direct analysis of the interaction(s) between D2-containing endosomes and the ~88-kDa globular tail of myosin V showed that T_4 promoted the direct binding of this polypeptide to the D2 vesicle.

Deletion analysis and antibody inhibition studies localized the vesicle-tethering domain to the COOH-terminal 21 amino acids of the motor protein. Using a series of progressively truncated myosin V^{tail} polypeptides that cannot bind to F-actin, the T_4-dependent binding of endosomes to F-actin was specifically blocked, presumably by competition with endogenous myosin V for the D2 vesicles. The demonstration of a direct T_4-dependent interaction between an exogenous myosin V^{tail} and the p29 endocytotic vesicle *in situ* indicates that the *in vitro* binding assay faithfully mimicked the events taking place in the cell.

Based on the results obtained with our actin-binding assay, the COOH terminus of myosin V appears to play a key role in the tethering of endocytotic vesicles. The globular tail region of the myosin V is highly conserved from fly to human (16). In mice, the loss of the COOH-terminal 13 amino acids leads to phenotypic defects in cargo binding (16, 33) that are similar, if not identical, to the loss of vesicle binding observed with our myosin V deletion mutants *in vitro*. Interestingly, mice homozygous for the Myo5a^{d-n} mutation that lack the last 14 amino acids of the myosin V and show neurological defects between days 14 to 21 of life that are similar to those of the *dilute lethal* mouse (33). Similarly, mice carrying the Myo5a^{d-n2J}, a mutation that eliminates up to 92 amino acids from the myosin V tail, also show severe neurological defects during neonatal life; however, unlike the *dilute lethal* mouse, both the Myo5a^{d-n} and the Myo5a^{d-n2J} mouse survive and show improved neurological function in adults. Such a delay in the developmental program of the brain is similar to the delays in brain maturation associated with neonatal hypothyroidism (34, 35).

Our studies show that myosin V plays a major role in the thyroid hormone-dependent, actin-based endocytosis of D2. *In vivo*, myosin V is abundant in nerve terminals in brain, where it associates with synaptic vesicles (23, 24, 36). Biochemical analysis showed that the synaptic vesicle proteins, synaptobrevin and synaptophysin, formed calcium-dependent complexes with myosin V (14), whereas ultrastructure analysis revealed that myosin V decorated the larger SV2-containing vesicles in the nerve terminal (15), *i.e.* a vesicle pool formed of recycling synaptic vesicles (16). These data suggest that myosin V plays a significant role in actin-based endocytosis of synaptic vesicles at the nerve terminal.

In cAMP-stimulated astrocytes, thyroid hormone-dependent endocytosis of the D2-containing vesicles does not require intact microtubules (4). Importantly, the interplay between microtubule-based and microfilament-based motors is central to the function of myosin V in brain. Although the microtubule motor kinesin mediates axonal translocation of myosin V and its associated vesicles to the nerve terminal (30, 37), the dy-

namic, T_4-dependent regulation of D2 does not require intact microtubules, indicating that this is solely an actin-based endocytotic event. Interestingly, two of the four myosin V[tail] deletion mutants retain the kinesin binding AF-6 domain (38), and they were less effective competitors for D2 vesicles than deletion mutants lacking this domain. Because endogenous kinesins can interact with the AF-6 domain even in the absence of microtubules, it seems probable that the binding of kinesins to this domain on the MyoV[tail] and MyoV[1513] mutants could partially mask the COOH-terminal tethering domain and thereby decrease their ability to compete for D2 vesicles. Elimination of the AF-6 domain produced deletion mutants that were very potent competitors for D2 vesicles. These data suggest that the vesicle-tethering domain is distinct from the AF-6 domain.

Although it is clear that myosin V tethers vesicles to the actin cytoskeleton in a T_4-dependent manner, myosin V does not bind T_4. These data suggest that at least one additional T_4 binding protein is required and that its iodothyronine specificity and affinity are known. It is likely that this hormone-dependent linker protein is one of the accessory proteins bound to purified myosin V, because the interactions between detergent-insoluble lipid rafts and myosin V are mediated by protein complexes (39). On the other hand, vesicle-based docking protein(s) that expose a myosin V binding domain upon ligand binding is equally plausible. Importantly, our characterization of a specific region of myosin V used in this hormone-induced tethering event provides a powerful tool for identification and characterization of the putative, T_4-binding docking protein.

In summary, we have shown that myosin V mediates the T_4-dependent binding of primary endosomes to the actin cytoskeleton in preparation for internalization of the vesicle cargo. We also mapped the vesicle-binding region of myosin V to the most COOH-terminal part of the molecule. This is the first demonstration of a specific, hormone-regulated interaction between endocytotic vesicles and an actin-based motor protein.

REFERENCES

1. Leonard, J. L., Mellen, S. A., and Larsen, P. R. (1983) *Endocrinology* **112,** 1153–1155
2. Visser, T. J., Leonard, J. L., Kaplan, M. M., and Larsen, P. R. (1982) *Proc. Natl. Acad. Sci. U. S. A.* **79,** 5080–5084
3. Leonard, J. L., Silva, J. E., Kaplan, M. M., Mellen, S. A., Visser, T. J., and Larsen, P. R. (1984) *Endocrinology* **114,** 998–1004
4. Leonard, J. L., Siegrist-Kaiser, C. A., and Zuckerman, C. J. (1990) *J. Biol. Chem.* **265,** 940–946
5. Farwell, A. P., Lynch, R. M., Okulicz, W. C., Comi, A. M., and Leonard, J. L. (1990) *J. Biol. Chem.* **265,** 18546–18553
6. Silva, J. E., and Leonard, J. L. (1985) *Endocrinology* **116,** 1627–1635
7. Siegrist-Kaiser, C. A., Juge-Aubry, C., Tranter, M. P., Ekenbarger, D. M., and Leonard, J. L. (1990) *J. Biol. Chem.* **265,** 5296–5302
8. Farwell, A. P., DiBenedetto, D. J., and Leonard, J. L. (1993) *J. Biol. Chem.* **268,** 5055–5062
9. Farwell, A. P., Safran, M., Dubord, S., and Leonard, J. L. (1996) *J. Biol. Chem.* **271,** 16369–16374
10. Farwell, A. P., and Leonard, J. L. (1992) *Endocrinology* **131,** 721–728
11. Cheney, R. E., and Mooseker, M. S. (1992) *Curr. Opin. Cell Biol.* **4,** 27–35
12. Mermall, V., Post, P. L., and Mooseker, M. S. (1998) *Science* **279,** 527–533
13. Mooseker, M. S., and Cheney, R. E. (1995) *Annu. Rev. Cell Dev. Biol.* **11,** 633–675
14. Prekeris, R., and Terrian, D. M. (1997) *J. Cell Biol.* **137,** 1589–1601
15. Evans, L. L., Lee, A. J., Bridgman, P. C., and Mooseker, M. S. (1998) *J. Cell Sci.* **111,** 2055–2066
16. Reck-Peterson, S. L., Provance Jr., D. W., Mooseker, M. S., and Jercer, J. A. (2000) *Biochim. Biophys. Acta* **1496,** 36–51
17. Köhrle, J., Rasmussen, U. B., Ekenbarger, D. M., Alex, S., Rokos, H., Hesch, R. D., and Leonard, J. L. (1990) *J. Biol. Chem.* **265,** 6155–6163
18. Leonard, J. L. (1988) *Biochem. Biophys. Res. Commun.* **151,** 1164–1172
19. Laemmli, U. K. (1970) *Nature* **227,** 680–685
20. Leonard, D. M., Stachelek, S. J., Safran, M., Farwell, A. P., Kowalik, T. F., and Leonard, J. L. (2000) *J. Biol. Chem.* **275,** 25194–25201
21. Farwell, A. P., and Leonard, J. L. (1989) *J. Biol. Chem.* **264,** 20561–20567
22. Nascimento, A. A. C., Cheney, R. E., Tauhata, S. B. F., Larson, R. E., and Mooseker, M. S. (1996) *J. Biol. Chem.* **271,** 17561–17569
23. Mani, F., Espreafico, E. M., and Larson, R. E. (1994) *Braz. J. Med. Biol. Res.* **27,** 2639–2643
24. Tabb, J. S., Molyneaux, B. J., Cohen, D. L., Kuznetsov, S. A., and Langford, G. M. (1998) *J. Cell Sci.* **111,** 3221–3234
25. Langford, G. M., and Molyneaux, B. J. (1998) *Brain Res.* **28,** 1–8
26. Huang, J. D., Cope, M. J., Mermall, V., Strobel, M. C., Kendrick-Jones, J., Russell, L. B., Mooseker, M. S., Copeland, N. G., and Jenkins, N. A. (1998) *Genetics* **148,** 1951–1961
27. Catlett, N. L., and Weisman, L. S. (1998) *Proc. Natl. Acad. Sci. U. S. A.* **95,** 14799–147804
28. Wei, Q., Wu, X., and Hammer 3rd, J. A. (1997) *J. Muscle Res. Cell Motil.* **18,** 517–527
29. Evans, L. L., Hammer, J., and Bridgman, P. C. (1997) *J. Cell Sci.* **110,** 439–449
30. Bridgman, P. C. (1999) *J. Cell Biol.* **146,** 1045–1060
31. Wu, X., Bowers, B., Rao, K., Wei, Q., and Hammer, J. (1998) *J. Cell Biol.* **143,** 1899–1918
32. Wang, F., Chen, L., Arcucci, O., Harvey, E. V., Bowers, B., Xu, Y., Hammer, J. A. III, and Sellers, J. R. (2000) *J. Biol. Chem.* **275,** 4329–4335
33. Huang, J. D., Mermall, V., Strobel, M. C., Russell, L. B., Mooseker, M. S., Copeland, N. G., and Jenkins, N. A. (1998) *Genetics* **148,** 1963–1972
34. Porterfield, S. P., and Hendrich, C. E. (1993) *Endocr. Rev.* **14,** 94–106
35. Oppenheimer, J. H., and Schwartz, H. L. (1997) *Endocr. Rev.* **18,** 462–475
36. Mehta, A. D., Rock, R. S., Rief, M., Spudich, J. A., Mooseker, M. S., and Cheney, R. E. (1999) *Nature* **400,** 590–593
37. Huang, J. D., Brady, S. T., Richards, B. W., Stenolen, D., Resau, J. H., Copeland, N. G., and Jenkins, N. A. (1999) *Nature* **397,** 267–270
38. Ponting, C. P. (1995) *Trends Biochem. Sci.* **20,** 265–266
39. Miller, K. E., and Sheetz, M. P. (2000) *J. Biol. Chem.* **275,** 2598–2606